Copyright © 2009 Tech Science Press SL, vol.2, no.3, pp.157-168, 2009

Correlation of Crack Initiation Parameters with Life Estimation for Very-High-Cycle Fatigue of High Strength Steels

Chengqi Sun[1], **Aiguo Zhao**[1] **and Youshi Hong**[1,2]

Abstract: The researches on the behavior of very-high-cycle fatigue (VHCF) for high strength steels have become a new branch in the field of metal fatigue since 1980s. The characteristics of crack initiation and propagation for high strength steels in VHCF regime differ from those in low cycle regime. One of the most distinct phenomena for VHCF regime is the interior or subsurface crack initiation at inclusions or at other inhomogeneities. This paper attempts to further investigate the crack initiation with the morphology of so-called fish-eye and fine granular area (FGA) or optical dark area (ODA) for high strength steels. Fatigue tests were carried out on a high carbon low alloy steel by using rotating bending (52.5 Hz) and ultrasonic push-pull (20 kHz) machines and the fatigue fracture surfaces were examined by scanning electron microscopy. The present results showed the data of the stress intensity factor range (SIF) as a function of the dimension for FGA. Based on the present results and the ones from literature, two models are developed. One is to estimate the threshold value for FGA by taking into account the size of plastic zone at crack tip in relation with the value of SIF at FGA, and the other is to estimate the fatigue life by considering the fatigue damage cumulative process in relation with the microscopic parameters (inclusion size and FGA size) at the fracture region along with macroscopic quantities (tensile strength and stress level). The estimations are in good agreement with experimental results.

Keywords: Very-high-cycle fatigue, high strength steels, crack initiation, fatigue life estimation, FGA.

1 Introduction

The researches on the behavior of very-high-cycle fatigue (VHCF) for high strength steels have become a new branch in the field of metal fatigue since 1980s [Naito,

[1] LNM, Institute of Mechanics, Chinese Academy of Sciences, Beijing, China
[2] Correspondence author. E-mail: hongys@imech.ac.cn

Ueda, and Kikuchi (1983, 1984); Murakami, Nomoto, and Ueda (1999, 2000); Bathias, Drouillac, and Le Francois (2001); Paris, Marines-Garcia, Hertzberg, and Donald (2004); Hong, Zhao, and Qian (2009); Qian, Zhou, and Hong (2011)]. Different from the low cycle fatigue, a fish-eye fracture mode often presented for VHCF of high strength steels, and a fine granular area (FGA) [Sakai (2009)], also called optical dark area (ODA) [Murakami, Nomoto, and Ueda (1999)] or granular-bright-facet (GBF) [Shiozawa, Lu, and Ishihara (2001)] was observed surrounding the inclusion at the fracture origin in most cases. Sakai, Sato, Nagano, Takeda, and Oguma (2006) showed that the value of stress intensity factor range (SIF) at FGA corresponded to the threshold value of the crack propagation, and the value of SIF at the front edge of the fish-eye corresponded to the threshold value of the crack from stable propagation to unstable propagation. Due to the difficulty in understanding well the mechanism of FGA formation, some methods were proposed to study the fatigue life or fatigue strength in VHCF [Tanaka and Akiniwa (2002); Chapetti, Tagawa, and Miyata (2003); Harlow, Wei, Sakai, and Oguma (2006)]. For example, Murakami and Endo (1994) proposed $\sqrt{area}$ parameter model to predict the fatigue strength of high strength steels. Wang, Bathias, Kawagoishi, and Chen (2002) presented a model for predicting the fatigue life of high strength low alloy steels by developing the dislocation model for fatigue crack initiation proposed by Tanaka and Mura (1981) and using Paris law for the crack growth life.

Many researches have shown that the fatigue life of high strength steels in VHCF is primarily caused by the crack initiation stage, and more than 90% of fatigue life is spent on forming FGA [Wang, Bathias, Kawagoishi, and Chen (2002); Tanaka and Akiniwa (2002); Shiozawa, Morii, Nishino, and Lu (2006)]. According to the work by Murakami, Nomoto, and Ueda (1999), the crack growth rate was less than 10^{-11}m/cycle in the early stage of VHCF process, and one could not assume that crack growth occurred cycle by cycle. Hence, it is very essential to investigate the characteristics of FGA at the fracture region and to develop a model for estimating the fatigue life of FGA, in order to predict the fatigue life of mechanical components.

In this paper, a high carbon low alloy steel was tested with rotating bending and ultrasonic fatigue testing machines to investigate the characteristics of FGA. Based on the present results and the ones from literature, two models are developed. One is to estimate the threshold value for FGA, and the other is to estimate the fatigue life of high strength steels in VHCF regime. The estimation results are in good agreement with experimental results.

2 Experimental material and testing methods

The material used in the present paper is a high carbon low alloy steel (equivalent to AISI 5140 or SCr 440), and the main chemical compositions are 1.01C and 1.45Cr in mass percentage (Fe balance). The geometries of specimens are shown in Fig. 1. Specimens were heated at 845°C for 2 hours in vacuum, then oil-quenched and tempered for 2.5 hours in vacuum at 300°C with furnace-cooling. The tensile strength of specimens is 2150 MPa, and the Vickers hardness is 741 kgf/mm^2. The elastic stress concentration factor is 1.06 for rotating bending testing specimens. Before fatigue testing, the round notch surface was ground and polished to eliminate machine scratches.

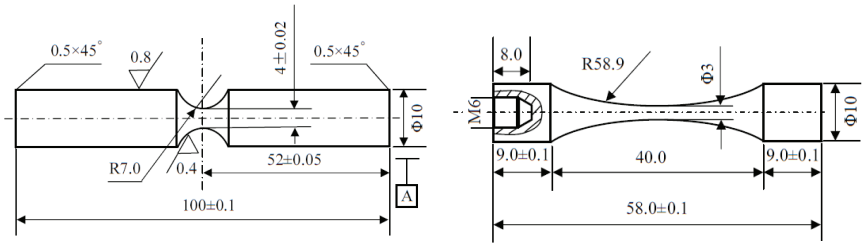

(a) Rotating bending fatigue test specimen (b) Ultrasonic fatigue test specimen

Figure 1: Geometries of specimens, dimensions in mm

Fatigue tests were carried out at room temperature in air by using a four-axis cantilever-type rotating bending machine (52.5 Hz) and a Shimadzu USF-2000 (20 kHz) with a resonance interval of 100 ms per 500 ms, respectively. The stress ratios were both $R = -1$, and compressive cold air was used to cool the specimens during ultrasonic fatigue testing. The fracture surfaces of all failed specimens were examined by scanning electron microscopy.

3 Experimental results

Most of the specimens failed from the interior-initiated fracture mode and a fish-eye pattern was shown, as illustrated in Figs. 2 and 3. The testing data of fatigue life with the values of inclusion and FGA observed on fracture surfaces are listed in Tab. 1. From Tab. 1, it is seen that the fatigue life is related to the inclusion size and the FGA size, indicating that the inclusion size and the FGA size at the fracture region play an important role in VHCF of high strength steels. Fatigue is a process of the accumulation of damage cycle by cycle in a material subjected to cyclic

stress and strain. Therefore, for fish-eye mode failure observed, the microscopic parameters (such as inclusion size and FGA size) at the fracture region should have an inherent relationship with the macroscopic quantities (the tensile strength and the stress level) based on the continuum mechanics concept.

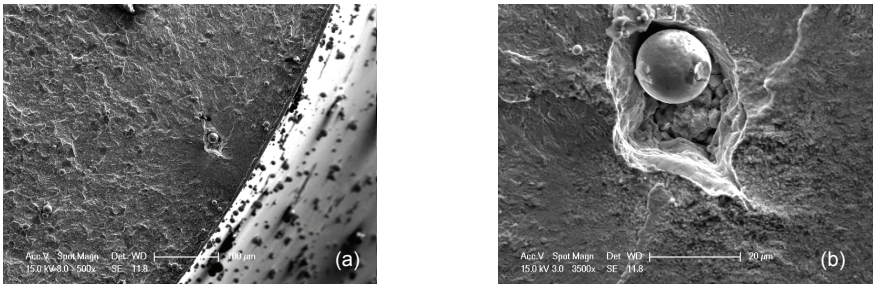

Figure 2: Fracture surface morphology for a broken specimen with a fish-eye pattern under rotating bending test, $\sigma = 675$ MPa, $N_f = 9.01 \times 10^7$. (a) Low magnification for fracture surface with fish-eye; (b) High magnification for FGA surrounding inclusion in the center of fish-eye

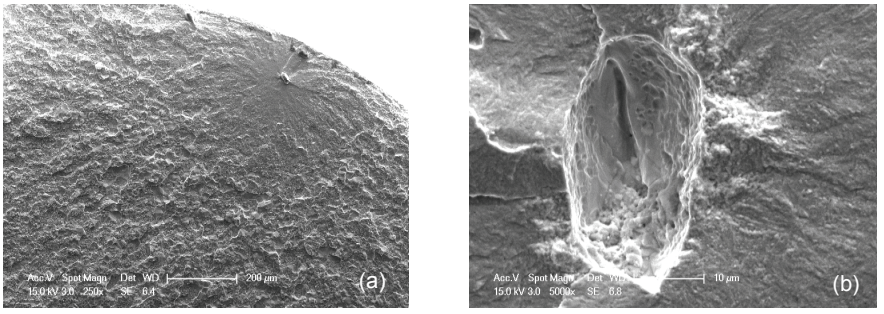

Figure 3: Fracture surface morphology for a broken specimen with a fish-eye pattern under ultrasonic test, $\sigma = 988$ MPa, $N_f = 9.40 \times 10^8$. (a) Low magnification for fracture surface with fish-eye; (b) High magnification for FGA surrounding inclusion in the center of fish-eye

Figure 4 shows the SIF at FGA ΔK_{FGA}, versus the fatigue life for the experimental results, in which ΔK_{FGA} is calculated by $\Delta K_{\mathrm{FGA}} = 0.5\sigma_a\sqrt{\pi\sqrt{area_{\mathrm{FGA}}}}$ [Murakami, Kodama, and Konuma (1988)], where σ_a is the stress amplitude. It is seen from Fig. 4 that the SIF at FGA is almost independent of fatigue life. It keeps almost

Table 1: Data of fatigue strength and crack origins measured from fracture surfaces

Rotating bending fatigue test					Ultrasonic fatigue test				
Specimen number	σ (MPa)	$\sqrt{area_{\mathrm{In}}}$ (μm)	$\sqrt{area_{\mathrm{FGA}}}$ (μm)	Fatigue life	Specimen number	σ (MPa)	$\sqrt{area_{\mathrm{In}}}$ (μm)	$\sqrt{area_{\mathrm{FGA}}}$ (μm)	Fatigue life
1	879	13.67	28.11	9.81×10^{6}	1	1148	16.82	28.41	5.75×10^{5}
2	855	25.02	39.76	9.68×10^{6}	2	1100	22.96	33.99	5.25×10^{5}
3	829	10.54	30.32	9.38×10^{7}	3	1074	20.35	32.76	1.08×10^{6}
4	806	54.77	70.26	9.99×10^{6}	4	1023	32.74	40.56	1.05×10^{6}
5	675	25.92	51.27	9.01×10^{7}	5	1008	18.49	30.68	3.50×10^{6}
					6	1000	28.60	41.48	8.18×10^{5}
					7	998	23.60	41.19	1.09×10^{7}
					8	994	22.38	37.79	5.35×10^{6}
					9	988	23.75	32.63	9.40×10^{8}
					10	986	26.06	33.69	2.19×10^{6}
					11	978	22.69	30.51	4.27×10^{7}
					12	960	37.80	45.16	2.04×10^{7}
					13	938	25.51	40.22	4.25×10^{6}

a constant, namely that the SIF at FGA reflects the basic fatigue property of high strength material. This result accords with the one for a high carbon chromium steel (SUJ2) in literature [Sakai, Sato, Nagano, Takeda, and Oguma (2006); Sakai (2009)].

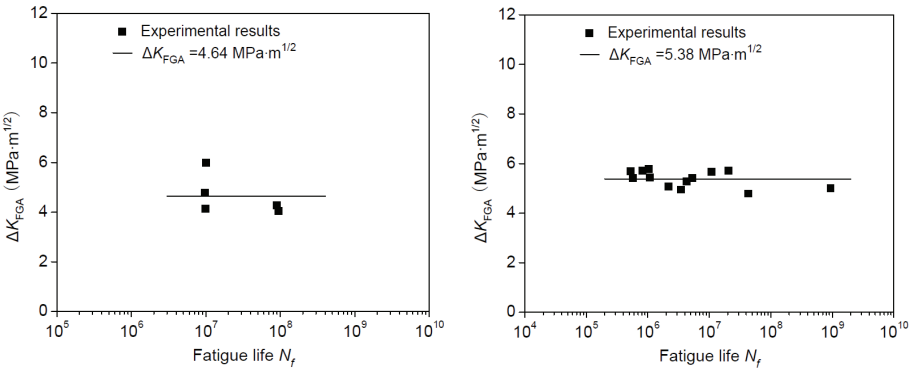

(a) Rotating bending fatigue test (b) Ultrasonic fatigue test

Figure 4: SIF at FGA versus fatigue life for experimental results

4 Estimation of the threshold value for FGA

The interior crack of FGA zone is considered under plain strain condition. For mode-I crack, the plastic zone size at the crack tip under plain strain condition is [Fan (2003)]

$$r_{\mathrm{p}} = \frac{(1-2\nu)^2}{\pi}\left(\frac{\Delta K}{\sigma_y}\right)^2 \approx \frac{1}{6\pi}\left(\frac{\Delta K}{\sigma_y}\right)^2 \tag{1}$$

According to the work by Nix and Gao (1998), the characteristic size of a material is

$$l_m = b\left(\frac{\mu}{\sigma_y}\right)^2 \tag{2}$$

where b is the Burgers vector, μ is the shear modulus, and σ_y is the yield strength. In this paper, it is assumed that when the plastic zone size of a crack equals to the width of martensite lamella (around 378 nm for the present steel) of the material, the formation of FGA is completed. Thus we have

$$\Delta K_{\mathrm{FGA}} = \mu\sqrt{6\pi b} \approx 4.342\mu\sqrt{b} \tag{3}$$

For steels, the SIF at FGA is calculated as 5.54 MPa·m$^{1/2}$, which is in good agreement with the average value of experimental results 4.64 MPa·m$^{1/2}$ under rotating bending test and 5.38 MPa·m$^{1/2}$ under ultrasonic test for SIF at FGA, and the value of SIF at FGA in the range of 4∼6 MPa·m$^{1/2}$ in literature [Shiozawa, Morii, Nishino, and Lu (2006)]. In addition, it is seen that the value of SIF at FGA by Eq.3 is independent of the material strength and hardness.

The model can explain the morphology of FGA quite different from the conventional fatigue fracture surface. In FGA zone, crack propagation distance per cycle is lower than martensite lamella width, so crack propagates in all directions, searches for the most favorable path, and leaves a rough fracture surface. In fish-eye zone outside FGA, crack propagation distance per cycle is larger than the width of martensite lamella, crack propagates in one direction and shows a smooth fracture surface.

5 Fatigue life estimation

5.1 Model and analysis

It is assumed that fish-eye mode failure presents for high strength steels in VHCF regime, and an FGA can be observed surrounding the inclusion at the fracture region. From the view of fatigue damage accumulation, the fatigue life of FGA is the minimum of integral N that satisfies

$$area_{\mathrm{In}} + \sum_{n=1}^{N} S_n \geq area_{\mathrm{FGA}} \tag{4}$$

where $area_{\mathrm{In}}$ is inclusion projection area, $area_{\mathrm{FGA}}$ is FGA, and S_n (n=1, 2, …, N) is the irreversible fatigue damage projection area surrounding the inclusion at crack initiation region due to the n th cycle.

Since $area_n = area_{n-1} + S_n$, note $p_n = S_n/area_{n-1}$, we have $area_n = area_{n-1}(1 + p_n)$. Therefore, Eq. 4 can be expressed as

$$area_N = area_{\mathrm{In}} \prod_{n=1}^{N} (1 + p_n) \geq area_{\mathrm{FGA}} \tag{5}$$

where $area_n$ is the total area of irreversible fatigue damage after n cycle, with $area_0 = area_{\mathrm{In}}$, and n=1, 2, …, N.

Note that $1 + p = \left[\prod_{n=1}^{N} (1 + p_n) \right]^{1/N}$, Eq.5 is changed to the following form

$$area_{\mathrm{In}} (1 + p)^N \geq area_{FGA} \tag{6}$$

From Eq.6, the fatigue life N_f contributed by FGA is solved approximately as

$$N_f \approx \frac{1}{\log(1+p)} \log \frac{area_{\mathrm{FGA}}}{area_{\mathrm{In}}} \tag{7}$$

Note that $k = 1/\log(1+p)$, Eq.7 becomes

$$N_f \approx k \cdot \log \frac{area_{\mathrm{FGA}}}{area_{\mathrm{In}}} \tag{8}$$

With the consideration that the stress level is one of the uppermost factors influencing the fatigue life, thus the parameter k is thought to be related to the stress level σ. Figure 5 plots the comparison of experimental values of $\lg N_f - \lg\log(area_{\mathrm{FGA}} / area_{\mathrm{In}})$ as a function of the normalized stress $\sigma_{\mathrm{b}}/\sigma$ with the fitting results. It is seen from Fig. 5 that the relation between $\lg N_f - \lg\log(area_{\mathrm{FGA}} / area_{\mathrm{In}})$ and $\sigma_{\mathrm{b}}/\sigma$ can be well approximated by a linear relation. Thus, the fatigue life can be expressed in the following form

$$N_f = 10^{\alpha \frac{\sigma_{\mathrm{b}}}{\sigma}} \log \frac{area_{\mathrm{FGA}}}{area_{\mathrm{In}}} \tag{9}$$

where the parameter α can be obtained by fitting the experimental data.

It is seen from Eq.9 that the fatigue life increases with the decrease of stress level and with the increase of inclusion size. In addition, the fatigue life increases with the decrease of FGA size. It is noted that the total fatigue life is assumed to be consumed to form FGA in the present paper.

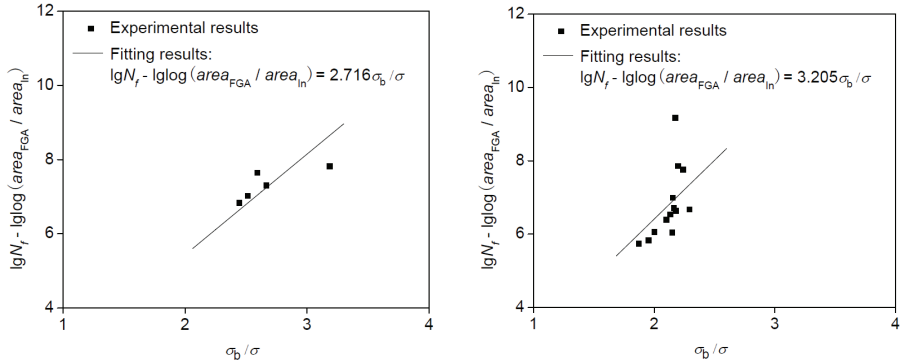

(a) Rotating bending fatigue test (b) Ultrasonic fatigue test

Figure 5: Experimental values of $\lg N_f - \lg\log(area_{\mathrm{FGA}} / area_{\mathrm{In}})$ versus normalized stress $\sigma_{\mathrm{b}}/\sigma$ with fitting results

5.2 Comparison with experimental results

Figure 6 shows the comparison of the fatigue life estimated by Eq.9 with the present experimental results, in which the FGA size is obtained from $\Delta K_{\mathrm{FGA}} = 0.5\sigma\sqrt{\pi\sqrt{area_{\mathrm{FGA}}}}$ according to the work by Murakami, Kodama, and Konuma (1988). The solid line denotes the fatigue life estimated by the present model with average inclusion size of specimens, the dashed line denotes the one estimated with minimum inclusion size of specimens, and the dotted line denotes the one estimated with maximum inclusion size of specimens. It is seen from Fig. 6 that the fatigue life estimated with the minimum inclusion size is generally higher than the experimental results, while the fatigue life estimated with the maximum inclusion size is generally smaller than the experimental results. The fatigue life estimated with average inclusion size is reasonably in good agreement with the experimental results, and most experimental datum points are within the range from the estimated values with the maximum inclusion size to the estimated ones with the minimum inclusion size. This indicates that the present model reflects the effect of inclusion size, and can be used to estimate the fatigue life of high strength steels in VHCF. Figure 6 also indicates that the inclusion size has an important influence on the fatigue life, and that the scatter of inclusion size is one of the most important factors resulting in the scatter of fatigue life. It is noted that, for the specimens with inclusion size bigger than the FGA size under a certain stress level, the present model is not valid for the estimation of fatigue life, and the corresponding results are not shown in the figure. In this study, we only consider the interior-initiated fracture mode with FGA observed surrounding the inclusion at the fracture region.

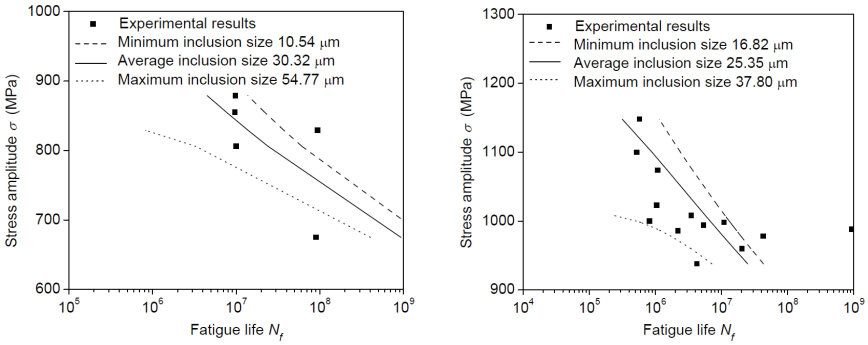

(a) Rotating bending fatigue test (b) Ultrasonic fatigue test

Figure 6: Comparison of fatigue life estimation with experimental results

6 Conclusions

In this paper, fatigue tests were carried out on a high carbon low alloy steel by using rotating bending and ultrasonic fatigue testing machines, and the fatigue fracture surfaces were examined by scanning electron microscopy. Based on the experimental results, the morphology of FGA is investigated, and a model is proposed to estimate the threshold value for FGA by considering the size of plastic zone at crack tip in relation with the value of SIF at FGA. Then, another model is developed to estimate the fatigue life of high strength steels containing VHCF regime by considering the fatigue damage cumulative process, which takes into account the inclusion size, FGA size, and tensile strength of materials. The estimation results are in good agreement with the experimental results.

Acknowledgement: The authors gratefully acknowledge the support of the National Natural Science Foundations of China (Grant Nos. 10721202 and 10772178) and the Knowledge Innovation Program of the Chinese Academy of Sciences (No. KJCX2-YW-L07).

References

Bathias, C.; Drouillac, L.; Le Francois, P. (2001): How and why the fatigue *S–N* curve does not approach a horizontal asymptote. *Int. J. Fatigue*, vol. 23, pp. S143–151.

Chapetti, M. D.; Tagawa, T.; Miyata, T. (2003): Ultra-long cycle fatigue of high-strength carbon steels part II: estimation of fatigue limit for failure from internal inclusions. *Mater. Sci. Eng. A*, vol. 356, pp. 236–244.

Fan T. Y. (2003): *Fracture Mechanics*. Beijing: Science Press. (in Chinese)

Harlow, D. G.; Wei, R. P.; Sakai, T.; Oguma, N. (2006): Crack growth based probability modeling of *S–N* response for high strength steel. *Int. J. Fatigue*, vol. 28, pp. 1479–1485.

Hong, Y.; Zhao, A.; Qian, G. (2009): Essential characteristic and influential factors for very-high-cycle fatigue behavior of metallic materials. *Acta Metall. Sinica*, vol. 45(7), pp. 769–780.

Murakami, Y.; Endo, M. (1994): Effects of defects, inclusions and inhomogeneities on fatigue strength. *Int. J. Fatigue*, vol. 16, pp. 163–182.

Murakami, Y.; Kodama, S.; Konuma, S. (1988): Quantitative evaluation of effects of nonmetallic inclusions on fatigue strength of high strength steel. *Trans. JSME*, vol. 54A, pp. 688–695.

Murakami, Y.; Nomoto, T.; Ueda, T. (1999): Factors influencing the mechanism

of superlong fatigue failure in steels. *Fatigue Fract. Eng. Mater. Struct.*, vol. 22(7), pp. 581–590.

Murakami, Y.; Nomoto, T.; Ueda, T. (2000): On the mechanism of fatigue failure in the superlong life regime (N>10^7 cycles). Part I: influence of hydrogen trapped by inclusions. *Fatigue Fract. Eng. Mater. Struct.*, vol. 23(11), pp. 893–902.

Naito, T.; Ueda, H.; Kikuchi, M. (1983): Observation of fatigue fracture surface of carburized steel. *J. Soc. Mater. Sci.*, vol. 32(361): pp. 1162–1166.

Naito, T.; Ueda, H.; Kikuchi, M. (1984): Fatigue behavior of carburized steel with internal oxides and nonmartensitic microstructure near the surface. *Metall. Trans. A*, vol. 15(7), pp. 1431–1436.

Nix, W. D.; Gao, H. J. (1998): Indentation size effects in crystalline materials: A law for strain gradient plasticity. *J. Mech. Phys. Solids*, vol. 46(3): pp. 411-425.

Paris, P. C.; Marines-Garcia, I.; Hertzberg, R.W.; Donald, J.K. (2004): The relationship of effective stress intensity, elastic modulus and Burgers vector on fatigue crack growth as associated with "fish-eye" gigacycle phenomena. *Proceedings of the Third International Conference on Very High-Cycle Fatigue*, pp. 1–13.

Qian, G.; Zhou, C.; Hong, Y. (2011): Experimental and theoretical investigation of environmental media on very-high-cycle fatigue behavior for a structural steel. *Acta Mater.*, vol. 59, pp. 1321–1327.

Sakai, T. (2009): Review and prospects for current studies on very high cycle fatigue of metallic materials for machine structural use. *Journal of Solid Mechanics and Materials Engineering*, vol. 3(3), pp. 425–439.

Sakai, T.; Sato, Y.; Nagano, Y.; Takeda, M.; Oguma, N. (2006): Effect of stress ratio on long life fatigue behavior of high carbon chromium bearing steel under axial loading. *Int. J. Fatigue*, vol. 28, pp. 1547–1554.

Shiozawa, K.; Lu, L.; Ishihara, S. (2001): *S–N* curve characteristics and subsurface crack initiation behaviour in ultra-long life fatigue of a high carbon–chromium bearing steel. *Fatigue Fract. Eng. Mater. Struct.*, vol. 24, pp. 781–790.

Shiozawa, K.; Morii, Y.; Nishino, S.; Lu, L. (2006): Subsurface crack initiation and propagation mechanism in high strength steel in a very high cycle fatigue regime. *Int. J. Fatigue*, vol. 28, pp. 1521–1532.

Tanaka, K.; Akiniwa, Y. (2002): Fatigue crack propagation behaviour derived from *S–N* data in very high cycle regime. *Fatigue Fract. Eng. Mater. Struct.*, vol. 25, pp. 775–784.

Tanaka, K.; Mura, T. (1981): A dislocation model for fatigue crack initiation. *J. Appl. Mech.* 48, pp. 97–103.

Wang, Q. Y.; Bathias, C.; Kawagoishi, N.; Chen, Q. (2002): Effect of inclusion

on subsurface crack initiation and gigacycle fatigue strength. *Int. J. Fatigue*, vol. 24, pp. 1269–1274.